JACS
JOURNAL OF THE AMERICAN CHEMICAL SOCIETY
Communication
pubs.acs.org/JACS

Substituent-Dependent Magnetic Behavior of Discotic Benzo[*e*][1,2,4]triazinyls

Marcin Jasiński,[†] Jacek Szczytko,[§] Damian Pociecha,[‡] Hirosato Monobe,[⊥] and Piotr Kaszyński*[,†,∥,¶]

[†]Faculty of Chemistry, University of Łódź, Tamka 12, 91-403 Łódź, Poland
[§]Institute of Experimental Physics, Faculty of Physics, University of Warsaw, Pasteura 5, 02-093 Warsaw, Poland
[‡]Department of Chemistry, University of Warsaw, Żwirki i Wigury 101, 02-089 Warsaw, Poland
[⊥]National Institute of Advanced Industrial Science and Technology (AIST), Kansai Centre, Ikeda, Osaka 563-8577, Japan
[∥]Center for Molecular and Macromolecular Studies, Polish Academy of Sciences, Sienkiewicza 112, 90-363 Łódź, Poland
[¶]Department of Chemistry, Middle Tennessee State University, Murfreesboro, Tennessee 37-132, United States

Supporting Information

ABSTRACT: Discotic mesogens containing the benzo[*e*][1,2,4]triazinyl radical as the central unit exhibit a Col_h phase below 80 °C. Depending on the substituent at the N(1) position, they show different modes of thermal expansion and magnetic behavior, presumably due to differences in molecular organization. Thus, for 1-phenyl (**1a**) and 1-PhF-*m* (**1b**) derivatives, the Col_h phase has positive thermal expansion coefficient κ and antiferromagnetic interactions, while for the 1-(3,4,5-$(C_{12}H_{25}X)_3C_6H_2$) derivatives **1c** (X = O) and **1d** (X = S), κ is negative and weak ferromagnetic interactions in the crystalline phase are observed for **1c** (J/k_B = +4.76 K). Compounds **1a** and **1c** exhibit photoinduced hole transport ($\mu \approx 1.3 \times 10^{-3}$ cm^2 V^{-1} s^{-1}) in the Col_h phase.

Self-organization of disc-like molecules with extended π electron systems into columns in a liquid crystalline phase has been recognized as an attractive method for obtaining materials that are of interest in developing organic field-effect transistors (OFETs),[1−3] organic light-emitting diodes (OLEDs),[4,5] and solar cells.[6−8] In contrast to typical aromatic structural elements,[9,10] π-delocalized radicals have smaller electrochemical windows and higher optical density in the visible range and, hence, exhibit higher photo- and electroactivity.[11] In addition, there has been growing interest in discotic radicals in the context of spintronics.[12]

In spite of progress in the chemistry of stable radicals,[11] discotic radicals are still rare.[12,13] Recently, we have reported discotic behavior of some verdazyl derivatives and their photovoltaic and magnetic properties.[14−16] In continuation of our search for new types of molecular and supramolecular arrangements and enhanced magnetic interactions of paramagnetic molecules, we focused on derivatives of the benzo[*e*][1,2,4]triazinyl radical. Relative to the verdazyl, benzo[*e*][1,2,4]triazinyl has more extended spin delocalization, smaller electrochemical window,[17] and its derivatives exhibit relatively strong antiferromagnetic,[18−22] ferromagnetic,[20,23−25] or both[26] types of interactions in the crystalline phase. Here we demonstrate the 1,4-dihydrobenzo[*e*][1,2,4]triazin-4-yl group as the central element of a disc-like molecular structure and investigate thermal, magnetic, and photovoltaic properties of the fluid phases of series **1a**−**1d**.

Radicals in series **1** (Scheme 1) were obtained in a typical yield of 40−70% using our recently developed method[27] by addition

Scheme 1. Synthesis of Benzo[*e*][1,2,4]triazinyl Derivatives[a]

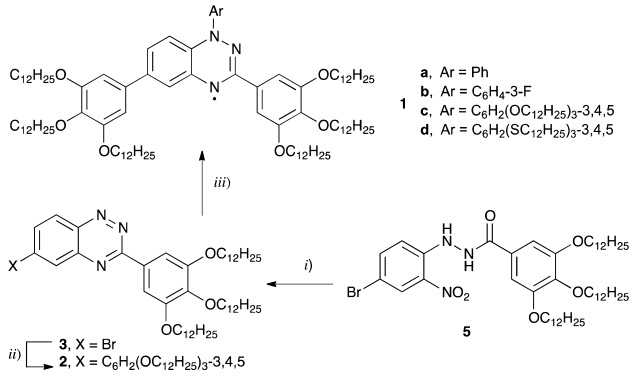

[a]Reagents and conditions: (i) 1) Sn, AcOH, rt 2 h, reflux 25 min, 2) $NaIO_4$, $MeOH/CH_2Cl_2$; (ii) 3,4,5-$(C_{12}H_{25}O)_3C_6H_2B(OH)_2$ (**4**), $Pd(PPh_3)_4$, K_2CO_3, THF/H_2O, reflux 24 h; (iii) 1) 3,4,5-$(C_{12}H_{25}O)_3C_6H_2Li$, THF, 2) air.

of ArLi to benzo[*e*][1,2,4]triazine **2**, followed by aerial oxidation of the intermediate anion. The triazine **2** was prepared by Suzuki coupling of 6-bromobenzo[*e*][1,2,4]triazine **3** with boronic acid **4** in 93% yield. The former was prepared in three steps and 63% overall yield from 3,4,5-tridodecyloxybenzhydrazide, which was *N*-arylated to form hydrazide **5** and subsequently cyclized to triazine **3**. Details are provided in the SI.

Electronic absorption and EPR spectroscopy and also electrochemical analyses demonstrated that substitution of the Blatter radical **I** (Figure 1) with 3,4,5-tridodecyloxyphenyl substituents has a modest effect on its electronic properties. Thus, placing two 3,4,5-$(C_{12}H_{25}O)_3C_6H_2$ groups in positions C(3) and C(6) of the benzo[*e*][1,2,4]triazinyl ring in **1a** lowers the oxidation potential of radical **I** by 0.06 V. Substitution of the

Received: June 22, 2016
Published: July 20, 2016

DOI: 10.1021/jacs.6b06444
J. Am. Chem. Soc. 2016, 138, 9421−9424

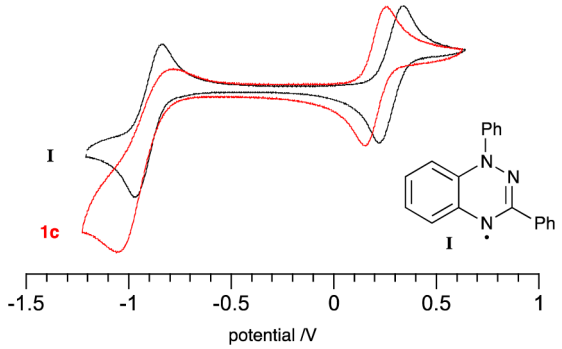

Figure 1. Cyclic voltammograms for Blatter radical **I** (black) and **1c** (red); 0.5 mM in CH_2Cl_2 $[n\text{-}Bu_4N]^+$ $[PF_6]^-$ (50 mM), at 20 °C, 100 mV s^{-1}, glassy carbon working electrode.

1-Ph in **1a** results in an additional shift of the oxidation potential according to the electronic effect of the substituent: cathodic for **1c** (−0.02 V, Figure 1) and anodic for **1b** (+0.01 V) and **1d** (+0.05 V).[28] In contrast to **I**, reduction of **1a**−**1d** is essentially irreversible, although the cathodic potential exhibits significant substituent dependence.[28]

EPR spectroscopy revealed similar patterns for all radicals **1** with *hfcc* essentially the same as for Blatter radical **I**. The 3,4,5-tridodecyloxyphenyl substituents move the $\pi-\pi^*$ transition of the Blatter radical **I** at 272 nm to lower energies ($\Delta E = 0.379$ eV) in **1c**, while absorption bands in the visible range gain intensity (hyperchromic shift, Figure 2).

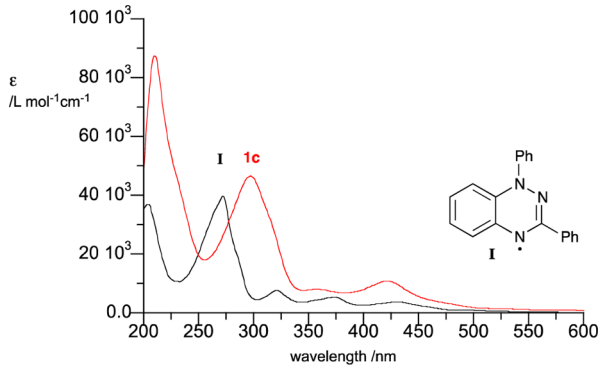

Figure 2. UV−vis spectra for Blatter radical **I** (black) and **1c** (red) in cyclohexane.

Thermal (Figure 3) and optical (Figure 4) analyses demonstrated that all derivatives **1** exhibit mesogenic behavior

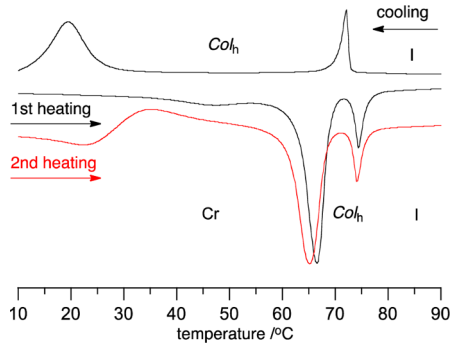

Figure 3. DSC trace of **1c**. The heating and cooling rates are 10 K min^{-1}.

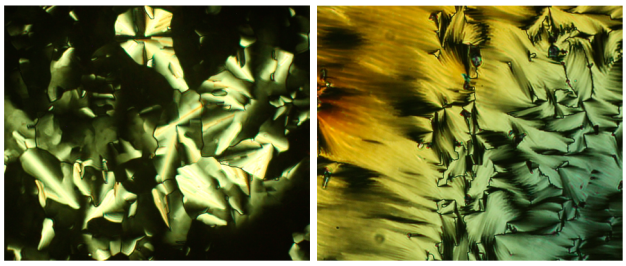

Figure 4. Optical textures of a Col_h phase obtained for **1c** upon cooling in 4 μm cell (left) and without top glass slide (right).

(Table 1), and regardless of the substituent at the N(1) position, all form a Col_h phase below 80 °C. Surprisingly, thermal stability

Table 1. Thermal Properties of 1[a]

	Ar	phase behavior
1a	Ph	Cr 46 (49.2) Col_h 73 (6.0) I
1b	C_6H_4-3-F	Cr 47 (46.1) Col_h 69 (2.5) I
1c	C_6H_2-3,4,5-$(OC_{12}H_{25})_3$	Cr 67 (84.6) Col_h 75 (13.9) I
1d	C_6H_2-3,4,5-$(SC_{12}H_{25})_3$	Cr 49 (47.8) Col_h 64 (11.6) I

[a]Cr = crystal; Col_h = columnar hexagonal; enthalpy of transition in parentheses (kJ mol^{-1}). Peak transition temperatures recorded for fresh samples on heating.

of the Col_h phase is essentially the same in derivatives with N(1)-Ph (**1a**) and N(1)-(3,4,5-$(C_{12}H_{25}O)_3C_6H_2$) (**1c**) substituents. The latter and also **1d** show tendency for glassification of the columnar phase (evident from the second heating cycle; Figure 3), which affects thermal and magnetic behavior of the sample (*vide infra*). Interestingly, the N(1)-unsubstituted triazine **2** does not exhibit liquid crystalline properties,[29] and only substitution at the N(1) position induces mesogenic behavior.

Powder XRD analysis confirmed the liquid crystalline phases formed by **1a**−**1d** as the Col_h phase: sharp, Bragg-type reflections at low angle range with positions in 1:$\sqrt{3}$:2 ratio evidence two-dimensional (2D) hexagonal lattice of columns (Figure 5). The

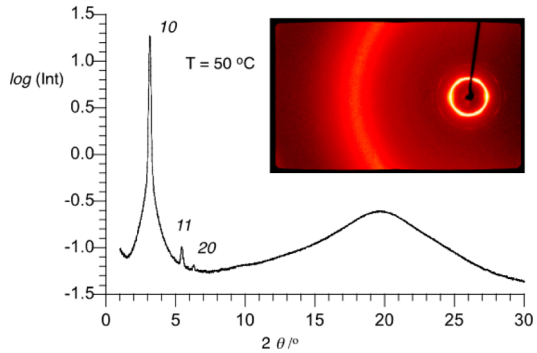

Figure 5. X-ray diffractogram for **1c** obtained by integration of the 2D pattern at 50 °C (inset): Col_h, a = 32.56 Å, diffused 4.5 and 3.7 Å.

column diameter, measured as a hexagonal lattice parameter a, corresponds to the dimension of a single molecule; it is larger by 2 Å for **1c** and **1d** with three 3,4,5-$(C_{12}H_{25}X)C_6H_2$ substituents than for **1a** and **1b**. The lattice parameter a shows a weak temperature dependence and changes by <3% over whole temperature range of the mesophase: it decreases on heating for compounds **1c** and **1d**, while for **1a** and **1b** it slightly increases. A broad diffused reflection in the high diffraction angle region can

DOI: 10.1021/jacs.6b06444
J. Am. Chem. Soc. 2016, 138, 9421−9424

be deconvoluted into two separate signals, which are indicative of a liquid-like positional correlation along the columns for both molecular cores and terminal chains. Interestingly, while for all compounds the mean distance between alkyl terminal chains is the same, 4.5 Å, there is significant difference in the mean distance between molecular cores: for **1a** and **1b** with small N(1) substituents the interdisc separation is 3.4 Å, while for compounds **1c** and **1d** with large N(1) substituents the distance increases to 3.7 and 3.9 Å, respectively (Table 2). The largest interdisc separation observed for **1d** can be attributed to the conformational properties of the alkylsulfanyl-aryl connection.[30]

Table 2. XRD Data for the Col_h Phase of 1

compd	temp (°C)	lattice parameter (Å)	diffuse (Å)
1a	60	a = 30.02	4.5, 3.4
1b	50	a = 30.05	4.5, 3.4
1c	70	a = 32.56	4.5, 3.7
1d	50	a = 32.30	4.5, 3.9

Magnetic susceptibility measurements of **1a**–**1c** revealed strong and diverse spin–spin interactions in the samples. The 1-phenyl derivative **1a** exhibits significant antiferromagnetic interactions in the isotropic phase, which upon cooling abruptly increases in the columnar phase and then completely dominates the crystalline phase (Figure 6). The $\chi_{para}T$ product in the

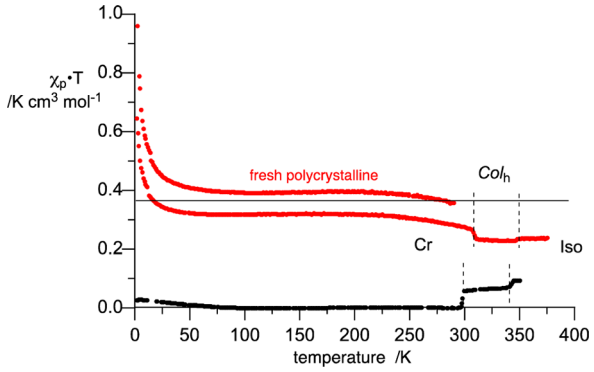

Figure 6. χ_p·T plot vs temperature for **1a** (black) and **1c** (red). Data obtained on cooling (0.8 K min^{-1}) at 0.2 and 0.1 T, respectively. The horizontal line marks the 0.375 value.

isotropic phase is about 0.094 cm^3·K·mol^{-1}, which is 25% of the Curie constant C = 0.375 cm^3·K·mol^{-1} for an ideal paramagnet with S = 1/2.[28] This free spin concentration drops to 18% in the Col_h phase and to <1% in the Cr phase. Qualitatively similar behavior is observed for the 1-(C_6H_4F-*m*) derivative **1b** with weaker antifferomagnetic interactions.

In contrast, **1c** and **1d** exhibit higher free spin content in the fluid phase, which increases upon crystallization. In addition, **1c** exhibits weak ferromagnetic interactions, which depends on the thermal history of the sample.

Pristine polycrystalline sample of **1c** showed paramagnetic behavior in the high-temperature range and the presence of ferromagnetic interactions between spins at lower temperatures, as evident from the upward turn of the $\chi_{para}T$ vs T plot (Figure 6). Assuming close π-stacked arrangements of molecules in the solid phase (similar to that in the Col_h) and hence 1D Heisenberg ferromagnetic chain model, magnetic susceptibility data were analyzed with Baker's high-temperature series expansion[31] to give the exchange interaction energy J/k_B = +4.76(1) K.[32]

In the fluid phase, **1c** exhibits antiferromagnetic interactions, which affect about one-third of the spins. Upon cooling of **1c** from the isotropic phase, antiferromagnetic interactions slightly increase in the Col_h phase and then abruptly decrease in the crystalline phase (Figure 6). The magnitude of this change at the Col_h–Cr transition in **1c** depends on the rate of cooling, which affects the extent of sample crystallization vs glassification of the Col_h phase.[28] Thus, for slowly cooled samples, 0.8 K min^{-1}, the number of free spins increase by ~20% at the Col_h–Cr transition, while essentially no change of magnetization occurs in fast cooled samples (10 K min^{-1}).[28] Similar behavior is observed for **1d** although with less pronounced increase of the spin content upon crystallization and weak antiferromagnetic interactions below 80 K.[28]

Magnetic behavior of derivatives **1** is vastly different from that observed in discotic derivatives of triphenylmethyl[13] and 6-oxoverdazyl,[14−16] in which spins are essentially isolated. Remarkably, all compounds **1** exhibit some antiferromagnetic interactions in fluid phases, but at the Col_h–Cr transition they undergo magnetic switching, which depends on the substituent at the N(1): **1a** and **1b** become antiferromagnetic similar to other paramagnetic liquids,[33,34] while the molecular structures of **1c** and **1d** impose different molecular arrangement in the crystal structure resulting in high spin concentration in both and ferromagnetic interactions in **1c**. These results suggest that microsegregation of the rigid and flexible parts (column formation) imposes cofacial π–π interactions, while the steric bulk of the N(1) substituent controls the proximity of the π systems and the mode of overlap of positive and negative spin densities and resulting from it types of magnetic interactions, according to the McConnell's model[35] (Figure 7). This interpretation is consistent with results of solid-state magneto-structural investigation of other benzo[*e*][1,2,4]triazinyls[18−26] and organic radicals in general.[11]

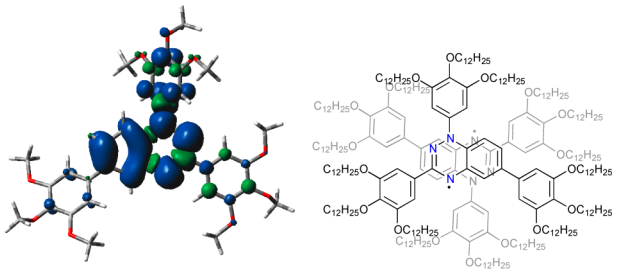

Figure 7. Spin density map for the all-methoxy analogue of **1c** (left) and proposed molecular arrangement in the columnar phase of **1c** (right).

Finally, time-of-flight (TOF) measurements found positive (hole) charge carrier mobilities (μ_h) in an partially homeotropically aligned samples of **1a** and **1c** to be nearly constant, 1.4 × 10^{-3} and 1.3 × 10^{-3} cm^2 V^{-1} s^{-1}, respectively, in a temperature range of 70 to 50 °C without electric field dependency. The measured mobility parameters fall in a typical range of 10^{-4}–10^{-1} cm^2 V^{-1}s^{-1}[10] and indicate microsegregation between the rigid molecular π cores and alkyl chains into channels in the Col_h phase.

In summary, we have demonstrated that benzo[*e*][1,2,4]-triazinyl is an effective spin-containing structural element of photoconductive discotic mesogens. Thus, substituting of the triazine **2** with either small or large aryl at the N(1) position induces Col_h behavior of radicals **1**. The radicals exhibit strong intermolecular spin–spin interactions, in which antiferromag-

DOI: 10.1021/jacs.6b06444
J. Am. Chem. Soc. 2016, 138, 9421−9424

netic interactions dominate in the fluid phase, while the type of interactions in the crystalline phase is controlled by the size of the aryl substituent at the N(1) position. The presented findings have significant implications for the development of new soft materials for molecular electronics and spintronics. Further experiments to explore this new class of mesogenic materials and to understand the origin of the observed magnetic effects are under way.

■ ASSOCIATED CONTENT

Supporting Information

The Supporting Information is available free of charge on the ACS Publications website at DOI: 10.1021/jacs.6b06444.

Full details of synthesis and characterization of compounds, NMR and EPR spectra, additional DSC, XRD, electrochemical, magnetization, photovoltaic, and computational details and results (PDF)

■ AUTHOR INFORMATION

Corresponding Author

*piotrk@cbmm.lodz.pl

Notes

The authors declare no competing financial interest.

■ ACKNOWLEDGMENTS

Dedicated to Professor Fred Wudl on the occasion of his 75th birthday. We thank Dr. S. Domagała of UŁ for help with e-chem measurements. This project was supported by the National Science Center (2013/09/B/ST5/01230, 2013/11/B/ST3/04193, 2014/13/B/ST5/04525) and National Science Foundation (CHE-1214104) grants.

■ REFERENCES

(1) Tsao, H. N.; Pisula, W.; Liu, Z.; Osikowicz, W.; Salaneck, W. R.; Müllen, K. *Adv. Mater.* **2008**, *20*, 2715.

(2) Oikawa, K.; Monobe, H.; Nakayama, K.-i.; Kimoto, T.; Tsuchiya, K.; Heinrich, B.; Guillon, D.; Shimizu, Y.; Yokoyama, M. *Adv. Mater.* **2007**, *19*, 1864.

(3) Zhang, F.; Funahashi, M.; Tamaoki, N. *Org. Electron.* **2010**, *11*, 363.

(4) Kogo, K.; Goda, T.; Funahashi, M.; Hanna, J.-i. *Appl. Phys. Lett.* **1998**, *73*, 1595.

(5) Tokuhisa, H.; Era, M.; Tsutsui, T. *Appl. Phys. Lett.* **1998**, *72*, 2639.

(6) Schmidt-Mende, L.; Fechtenkötter, A.; Müllen, K.; Moons, E.; Friend, R. H.; MacKenzie, J. D. *Science* **2001**, *293*, 1119.

(7) Schmidt-Mende, L.; Fechtenkötter, A.; Müllen, K.; Friend, R. H.; MacKenzie, J. D. *Phys. E* **2002**, *14*, 263.

(8) van de Craats, A. M.; Warman, J. M.; Fechtenkötter, A.; Brand, J. D.; Harbison, M. A.; Müllen, K. *Adv. Mater.* **1999**, *11*, 1469.

(9) Pisula, W.; Müllen, K. In *Hanbook of Liquid Crystals*; Goodby, J. W., Collings, P. J., Kato, T., Tschierske, C., Gleeson, H. F., Raynes, P., Eds.; Wiley-VCH: Mörlenbach, Germany, 2014; Vol. 8, pp 627−673.

(10) Kaafarani, B. R. *Chem. Mater.* **2011**, *23*, 378.

(11) *Stable radicals: fundamentals and applied aspects of odd-electron compounds*; Hicks, R. G., Ed.; John Wiley & Sons: Chichester, 2010.

(12) Ravat, P.; Marszalek, T.; Pisula, W.; Müllen, K.; Baumgarten, M. *J. Am. Chem. Soc.* **2014**, *136*, 12860.

(13) Castellanos, S.; López-Calahorra, F.; Brillas, E.; Juliá, L.; Velasco, D. *Angew. Chem., Int. Ed.* **2009**, *48*, 6516.

(14) Jankowiak, A.; Pociecha, D.; Szczytko, J.; Monobe, H.; Kaszyński, P. *J. Am. Chem. Soc.* **2012**, *134*, 2465.

(15) Jankowiak, A.; Pociecha, D.; Monobe, H.; Szczytko, J.; Kaszyński, P. *Chem. Commun.* **2012**, *48*, 7064.

(16) Jankowiak, A.; Pociecha, D.; Szczytko, J.; Kaszyński, P. *Liq. Cryst.* **2014**, *41*, 1653.

(17) Berezin, A. A.; Zissimou, G.; Constantinides, C. P.; Beldjoudi, Y.; Rawson, J. M.; Koutentis, P. A. *J. Org. Chem.* **2014**, *79*, 314.

(18) Constantinides, C. P.; Koutentis, P. A.; Rawson, J. M. *Chem. - Eur. J.* **2012**, *18*, 15433.

(19) Constantinides, C. P.; Berezin, A. A.; Manoli, M.; Leitus, G. M.; Bendikov, M.; Rawson, J. M.; Koutentis, P. A. *New J. Chem.* **2014**, *38*, 949.

(20) Constantinides, C. P.; Berezin, A. A.; Manoli, M.; Leitus, G. M.; Zissimou, G. A.; Bendikov, M.; Rawson, J. M.; Koutentis, P. A. *Chem. - Eur. J.* **2014**, *20*, 5388.

(21) Zheng, Y.; Miao, M.-s.; Kemei, M. C.; Seshadri, R.; Wudl, F. *Isr. J. Chem.* **2014**, *54*, 774.

(22) Miura, Y.; Yoshioka, N. *Chem. Phys. Lett.* **2015**, *626*, 11.

(23) Constantinides, C. P.; Koutentis, P. A.; Krassos, H.; Rawson, J. M.; Tasiopoulos, A. J. *J. Org. Chem.* **2011**, *76*, 2798.

(24) Yan, B.; Cramen, J.; McDonald, R.; Frank, N. L. *Chem. Commun.* **2011**, *47*, 3201.

(25) Takahashi, Y.; Miura, Y.; Yoshioka, N. *New J. Chem.* **2015**, *39*, 4783.

(26) Constantinides, C. P.; Berezin, A. A.; Zissimou, G. A.; Manoli, M.; Leitus, G. M.; Bendikov, M.; Probert, M. R.; Rawson, J. M.; Koutentis, P. A. *J. Am. Chem. Soc.* **2014**, *136*, 11906.

(27) Constantinides, C. P.; Obijalska, E.; Kaszyński, P. *Org. Lett.* **2016**, *18*, 916.

(28) For details see the Supporting Information.

(29) Transition temperatures (°C) and enthaplies (kJ mol^{-1}) for **2**: Cr_1 30 (*17.0*) Cr_2 80 (*47.1*) I.

(30) For results of molecular modeling of the 3,4,5-$(RS)_3C_6H_2$ and 3,4,5-$(RO)_3C_6H_2$ substituents see: Jankowiak, A.; Pociecha, D.; Szczytko, J.; Monobe, H.; Kaszyński, P. *Liq. Cryst.* **2014**, *41*, 385 and refs 14 and 15.

(31) Baker, G. A., Jr.; Rushbrooke, G. S.; Gilbert, H. E. *Phys. Rev.* **1964**, *135*, A1272.

(32) Thermally populated triplet states were recently reported in a columnar phase of a nitroxide derivative of hexabenzocoronene; ref 12.

(33) Brooks, W. V. F.; Burford, N.; Passmore, J.; Schriver, M. J.; Sutcliffe, L. H. *J. Chem. Soc., Chem. Commun.* **1987**, 69.

(34) Brownridge, S.; Du, H.; Fairhurst, S. A.; Haddon, R. C.; Oberhammer, H.; Parsons, S.; Passmore, J.; Schriver, M. J.; Sutcliffe, L. H.; Westwood, N. P. C. *J. Chem. Soc., Dalton Trans.* **2000**, 3365.

(35) McConnell, H. M. *J. Chem. Phys.* **1956**, *24*, 764.

DOI: 10.1021/jacs.6b06444
J. Am. Chem. Soc. 2016, 138, 9421−9424